This chapter provides a concise introduction to magnetization dynamics in single magnetic domains, with an emphasis on behavior in ferromagnetic metal thin films. The material presented here underpins micromagnetics, which writes coupled equations of motions for single magnetic domains, and spin torque, which adds additional terms to the equation of motion for a single domain.

In Section 1, I will provide motivation and formalism for the fundamental equation of motion of magnetization, the *Landau-Lifshitz (Gilbert) equation*, or LLG. Small-angle solutions of the LLG are developed in Section 2.1. I will emphasize how materials parameters have been extracted from experiments, particularly ferromagnetic resonance experiments, in Section2.2, and tabulate some materials parameters in Section 2.3. Approaches to calculate large-angle dynamics are developed in Section 3; I show quasistatic aspects of switching and a short example of how to integrate the nonlinear LLG for a switching experiment. Finally, in Section 4, I describe how spin torque terms modify the LLG equation and draw out some simple consequences.

Interested readers may wish to consult more focused, recent reviews on specific topics covered here: by Farle[1] on magnetic anisotropies in ultrathin films, by Russek[2] on electrical measurements of magnetization dynamics in sub-micron structures, by Heinrich[3] on the physical basis of ferromagnetic relaxation, by Stiles and Ralph[4] on spin transfer torque, and by Mayergoyz et al on nonlinear magnetization dynamics in nanosystems[5].

1 Landau-Lifshitz-Gilbert (LLG) equation

The Landau-Lifshitz-Gilbert equation for magnetization dynamics includes two types of motion, *precession* and *relaxation*. Historical context for the equation is given in Section 1.3. Section 1.3.1 shows how the LLG can be motivated intuitively through magnetomechanical experiments, and show how additional terms (such as those resulting from spin torque) can be added to the equation of motion. In Section 1.4, I show how the Landau Lifshitz (LL) and and Gilbert (LLG) damping terms are equivalent in terms of the resulting motion, and can be used interchangeably.

1.1 Introduction

Our direct experience with magnets tells us about the final state of magnetization dynamics. The magnetization $\mathbf{M}$ of a soft ferromagnetic material tends to align with applied magnetic fields $\mathbf{H}$: permanent magnets are attracted to an iron body, after their dipolar field has magnetized the iron underneath, and compass needles rotate towards and eventually come to rest along the earth's magnetic field. Both these examples illustrate that in the final state, the Zeeman energy

$$U = -\mathbf{M} \cdot \mathbf{H} \, (cgs) \qquad U = -\mu_0 \mathbf{M} \cdot \mathbf{H} \, (SI) \tag{1}$$

is minimized, where magnetization $\mathbf{M}$ and applied field $\mathbf{H}$ line up parallel.

Our experience might then lead us to guess then that the *full motion* of magnetic north and south poles, $\dot{\mathbf{M}}$, describes rotation along a direct, energy-minimizing path. However, the dynamics of magnetization $\dot{\mathbf{M}}$ have two terms rather than only one, and the energy-minimizing term, *relaxation*, is usually one or two orders of magnitude smaller than an energy-preserving term, the *precession*. For precessional motion only, no energy is lost; $U = -\mu_0 \mathbf{M} \cdot \mathbf{H_{eff}}$ remains constant as the magnetization $\mathbf{M}$ simply rotates around the field $\mathbf{H_{eff}}$. The precession and relaxation terms were written first by Landau and Lifshitz in their 1935 paper[6].

1.2 Variables in the equation

Before describing the LL equation, we define the variables involved, the choice of which contains important assumptions about the physics.

Reduced magnetization Ferromagnets are distinguished by their spontaneous magnetic order. For any magnetic material, the magnetization can be written as $M = N_v < \mu >$, where N_v is a volume density of dipole moments ($[=]\mathrm{m}^{-3}$) and $< \mu >$ is an ensemble average dipole moment ($[=]\mathrm{A{\cdot}m}^2$), taken along the direction of the applied field. The magnitude $|\mu|$ is constant in a ferromagnet, independent of applied field $\mathbf{H}$ for constant temperature. Within a single *domain,* the magnetization is equal to the saturation magnetization $M = M_s = N_v|\mu|$. The direction of $\mathbf{M}$ can vary; the influence of $\mathbf{H}$ is to change the direction. It becomes sensible to define the *reduced magnetization* $\mathbf{m}$

$$\mathbf{m} \equiv \mathbf{M}/M_s \tag{2}$$

as a unit vector of the magnetization direction. Magnetization dynamics are then *rotational,* at right angles to $\mathbf{m}$, describing trajectories on the unit sphere

$$\mathbf{m} \cdot \dot{\mathbf{m}} = 0 \tag{3}$$

Clearly, in ferromagnetic materials the demagnetized state $\mathbf{M} = 0$ is possible, but only as a large-scale average over domains, averaging to zero magnetization. Micromagnetic calculations make the similar assumption that in each finite element, $\mathbf{m}$ is a unit vector, M_s does not change, and the task is to calculate $\mathbf{m}(\mathbf{r})$ for all space $\mathbf{r}$.

Effective field The magnetization direction $\mathbf{m}$ influences the energy of a ferromagnet in several ways. The Zeeman energy (Eq 1)created by applied external fields $\mathbf{H_B}$ is one energy term, but the variation of $\mathbf{m}(\mathbf{r})$ can create other terms as well. Anisotropies due to shape (dipolar fields), interaction with crystal fields (magnetocrystalline anisotropy, induced anisotropy in alloys), stress, and exchange all have different possible energy terms. The most convenient way to treat these additional energies is through the definition of an *effective field*,

$$\mathbf{H^i_{eff}} = -\frac{1}{M_s}\frac{\partial U_i}{\partial \mathbf{m}}(cgs) \qquad \mathbf{H^i_{eff}} = -\frac{1}{\mu_0 M_s}\frac{\partial U_i}{\partial \mathbf{m}}(SI) \tag{4}$$

Since magnetic fields directed along $\mathbf{m}$ cannot rotate the magnetization, they are not effective. A cartesian basis for $\mathbf{H_{eff}}$ in three variables is thus less compact than a spherical basis:

$$\mathbf{H^i_{eff}} = -\frac{1}{\mu_0 M_s}\left(\frac{\partial U}{\partial m_x}\hat{\mathbf{x}} + \frac{\partial U}{\partial m_y}\hat{\mathbf{y}} + \frac{\partial U}{\partial m_z}\hat{\mathbf{z}}\right) \qquad \mathbf{H^i_{eff}} = -\frac{1}{\mu_0 M_s}\left(\frac{\partial U}{\partial \phi}\hat{\phi} + \frac{1}{\sin\phi}\frac{\partial U}{\partial \theta}\hat{\theta}\right) \tag{5}$$

where the derivative in r is not allowed. It is conventional to take the magnetization direction as $\hat{\mathbf{r}} = \sin\phi\sin\theta\hat{\mathbf{x}} + \cos\phi\sin\theta\hat{\mathbf{y}} + \cos\theta\hat{\mathbf{z}}$.

1.3 The equation

In LL's original paper, they propose the form[6]

$$\frac{\dot{\mathbf{M}}}{|\gamma|} = \mathbf{H_{eff}} \times \mathbf{M} + \lambda \left[\mathbf{H_{eff}} - \left(\frac{\mathbf{H_{eff}} \cdot \mathbf{M}}{{M_s}^2} \right) \mathbf{M} \right] (cgs) \tag{6}$$

in a slightly different nomenclature[1]. In the 75-odd years since LL's proposal, the equation stands uncorrected. Alternate forms proposed for the second (relaxation) term (see Section 1.4) turn out to be equivalent. The gyromagnetic ratio in this context is

$$\gamma = \frac{e}{2m_e} * g_{eff} \qquad \text{(SI)} \qquad \gamma = \frac{e}{2m_e c} * g_{eff} \qquad \text{(cgs)} \tag{7}$$

where e is the electronic charge, m_e is the electronic rest mass, and c is the speed of light. Numerically, this is most conveniently expressed as

$$\gamma = \gamma_0 \left(\frac{g_{eff}}{2} \right) \qquad \gamma_0^{cgs} = -2\pi \cdot 27.99 \text{ Ghz/T} \left(\frac{g_{eff}}{2} \right) \qquad \gamma_0^{SI} = -2\pi \cdot 2.799 \text{ Mhz/Oe} \left(\frac{g_{eff}}{2} \right) \tag{8}$$

with $g_{eff} = 2$, as LL considered pure-spin moments only. This assumption has been relaxed in subsequent years and values of g_{eff} up to 2.2 have been established experimentally given the mostly quenched, but nevertheless finite amounts of orbital moment present in magnetic materials[7]. See Section 2.3 for discussion.

Modern treatments of the LL equation typically use an alternate form, although the original form is no less valid and is used occasionally. Dividing Eq. 6 through by M_s, making use of the vector identity $\mathbf{a} \times \mathbf{b} \times \mathbf{c} = \mathbf{b}\,(\mathbf{a} \cdot \mathbf{c}) - \mathbf{c}\,(\mathbf{a} \cdot \mathbf{b})$, thus $-\mathbf{m} \times \mathbf{m} \times \mathbf{H_{eff}} = \mathbf{H} - \mathbf{m}\,(\mathbf{m} \cdot \mathbf{H_{eff}})$, and introducing the *dimensionless damping* α, we can write

$$\dot{\mathbf{m}} = -|\gamma| \mathbf{m} \times \mathbf{H_{eff}} - \alpha |\gamma| \left(\mathbf{m} \times \mathbf{m} \times \mathbf{H_{eff}} \right) (cgs) \tag{9}$$

$$\dot{\mathbf{m}} = -\mu_0 |\gamma| \mathbf{m} \times \mathbf{H_{eff}} - \alpha \mu_0 |\gamma| \left(\mathbf{m} \times \mathbf{m} \times \mathbf{H_{eff}} \right) (SI) \tag{10}$$

$$\lambda_{cgs} \equiv |\gamma| M_s \alpha \tag{11}$$

The value of λ, defined this way, is the same value in s^{-1} for both cgs and SI units, differing from the convention in Ref [8]. The parameter α is preferred by most authors and has the same value in the four combinations of unit system and damping form.

1.3.1 Precessional term

The first term of the LL equation is conservative. All energy stored in the magnetization system and its interactions with the lattice, expressed through the energy in the effective field, $U = -\mu_0 M_s \mathbf{m} \cdot \mathbf{H_{eff}}$, remains stored under operation of this term. Because the precessional term is dominant, constant-energy lines for $\mathbf{m}(\theta, \phi)$ can be a good approximation for trajectories.

The form for the precessional term can be derived from Eherenfest's theorem in quantum mechanics, as shown in elementary texts such as Liboff[9]. For observable x, the average time evolution is given by $< \dot{x} >= [x, \hat{H}]/i\hbar$; the Hamiltonian contains the spin through $\hat{H} = -\gamma \mu_0 \mathbf{B} \cdot \mathbf{s}$, and the transverse spin components oscillate as $\omega = \gamma B$. This form was natural for LL.[2] We will instead motivate the precessional term semiclassically, through the Einstein-de Haas experiments[10].

[1] $\mathbf{s} \leftrightarrow \mathbf{M}$ (spin magnetization), $\mu_0 \leftrightarrow |\gamma|$ (explicitly for $g_{eff} = 2$), $\mathbf{f} \leftrightarrow \mathbf{H_{eff}}$ for effective field, square brackets for cross products, parentheses for dot products, thus $\mathbf{s}/\mu_0 = [\mathbf{f}\,\mathbf{s}] + \lambda \left[1 - (\mathbf{f}\,\mathbf{s})\,\mathbf{s}/s^2 \right]$.

[2] Their addition of the *effective field* $\mathbf{f}$ was original and has been widely adopted since then.

Einstein-de Haas experiments Einstein showed–in his only experiments–that there is a real connection between magnetization **M** and angular momentum **L**. The magnetization of a cylinder of soft iron was suspended by a thin wire. An external solenoid coil, reversed the magnetization, changing it by $\Delta M = 2M_s$ along its axis. The reversal was seen to cause the cylinder rotate around its axis. The ratio between the mechanical angular momentum and magnetic angular momentum was indentified as γ, where $\Delta M = \gamma \Delta L$. This relation can be generalized to a dynamical equation. Taking the time derivative of both sides yields

$$\dot{\mathbf{M}} = \gamma\tau \qquad \dot{\mathbf{M}} = \gamma\mu_0 \mathbf{M} \times \mathbf{H} \tag{12}$$

where τ is a mechanical torque on the body. In the second expression, we substitute the torque on a point dipole per unit volume (magnetization) in a uniform field, $\tau = \mu_0 \mathbf{M} \times \mathbf{H}$, appropriate under the single domain approximation detailed already. Eq. 12 provides an alternate and surprising derivation of the first term in the LL equation not mentioned in [6].

Magnetomechanical values of γ were in reasonable agreement with the free-electron result e/m (e/mc cgs). It is remarkable that Einstein was able to carry out these experiments in his spare time while he developed the theory of relativity, although students with similar ambitions should be aware that his measurements were found to be in error by a factor of two[11]. Magnetomechanical and microwave resonance measurements of γ were later found by Barnett to agree within 10%[12], whose measurements continued into the early 1950s[13].

Additional torque terms Both the torque and the magnetic moment are total, volume-summed quantities, so to convert an additional torque term to dynamics of reduced magnetization **m**, the torque term needs to be expressed as

$$\dot{\mathbf{m}} = \ldots - \frac{|\gamma|}{StM_s}\tau(cgs) \qquad \dot{\mathbf{m}} = \ldots - \frac{|\gamma|}{St\mu_0 M_s}\tau(SI) \tag{13}$$

Here the volume of the film is taken as $S \cdot t$, where S is the area and t is the thickness.

1.4 Relaxation term

The relaxation term has been more controversial and more widely discussed in the years since LL's paper. LL added the term completely *ad-hoc* in order to direct the magnetization towards $\mathbf{H_{eff}}$. In the equivalent expression, Eq. 9, it is clear how relaxation operates geometrically: $\mathbf{m} \times \mathbf{H}$ is an axis about which **m** needs to rotate to bring the **m** and **H** into alignment, and **m** moves at right angles to it.

Gilbert form An alternate form for the damping was proposed by Gilbert in 1955[14], allowing the new LL equation to be written as

$$\dot{\mathbf{m}} = -|\gamma|\mathbf{m} \times \mathbf{H_{eff}} + \alpha \mathbf{m} \times \dot{\mathbf{m}}\,(cgs) \qquad \dot{\mathbf{m}} = -\mu_0|\gamma|\mathbf{m} \times \mathbf{H_{eff}} - \alpha \mathbf{m} \times \dot{\mathbf{m}}\,(SI) \tag{14}$$

This form is known as the *Landau-Lifshitz Gilbert* (LLG) equation. Gilbert justified the new damping term by claiming that the "higher" damping observed for $Ni_{81}Fe_{19}$ platelets would be better represented by a "viscous" term, proportional to $\dot{\mathbf{m}}$. For low damping, $\alpha \ll 1$ (true for almost all known cases), it can be shown easily that the LL and LL-G forms are equivalent. If the relaxation term to the motion is small compared with the precessional term, one can obtain Eq. 14 from Eq. 9 by substituting $\dot{\mathbf{m}} \simeq |\gamma|\mathbf{m} \times \mathbf{H_{eff}}$.

Functional equivalence of the LL and Gilbert damping The identity between the LL and LL-G forms is more exact than a small-damping approximation. Magnetization trajectories are equivalent for *all* dampings, *all* angles, subject to an inconsequential redefinition of γ. Decomposition of Eqs 10 and 14 into spherical coordinates yields the direct-integrable expressions

$$\begin{bmatrix} \dot{\theta} \\ \dot{\phi} \end{bmatrix} = \mu_0|\gamma| \begin{bmatrix} \alpha & 1 \\ -1/\sin\theta & \alpha/\sin\theta \end{bmatrix} \begin{bmatrix} H_\theta^{eff} \\ H_\phi^{eff} \end{bmatrix} \quad (SI, LL) \tag{15}$$

$$\begin{bmatrix} \dot{\theta} \\ \dot{\phi} \end{bmatrix} = \frac{\mu_0|\gamma|}{1+\alpha^2} \begin{bmatrix} \alpha & 1 \\ -1/\sin\theta & \alpha/\sin\theta \end{bmatrix} \begin{bmatrix} H_\theta^{eff} \\ H_\phi^{eff} \end{bmatrix} \quad (SI, LLG) \tag{16}$$

so that LL and LLG trajectories are *absolutely equivalent* if we take $\gamma_{LL} = \left(1+\alpha^2\right)^{-1}\gamma_{LLG}$. Gilbert recognized the equivalence in an expanded version of his paper published recently[15].

There can be no physical behavior that could be explained by the LLG that could not be explained by the LL, as long γ and α are both free parameters. The gyromagnetic ratio would need to be resolved to better than one part in α^{-2} to separate the expressions even in principle. Table 2.2 shows a best precision in measurements of γ to about 0.7%. While there may be formal reasons to prefer one form over another, a debate which continues[16], experimentalists have no reason to choose and can fit data to whichever form they prefer. The LL form is more convenient for algebraic manipulations since the right hand side contains no terms in $\dot{\mathbf{m}}$.

For completeness, we note that λ, a relaxation rate ($[=]\ s^{-1}$) in the LL damping scheme, has an analogue G in Gilbert damping. We can write

$$\lambda = \alpha\gamma_{cgs}M_s \qquad G = \alpha\gamma_{cgs}M_s \qquad \lambda = G \tag{17}$$

The literature on ferromagnetic relaxation uses *cgs* units, so this definition of λ is conventional; see Table 2.2 for values. If λ is expressed in terms of SI magnetizations

$$\lambda = G = \alpha\gamma_{SI}\frac{\mu_0 M_s}{4\pi} \tag{18}$$

2 Small-angle magnetization dynamics

In this section, we consider small-angle rotations of the magnetization for in-plane magnetization. First, in Section 2.1, we see how the LLG can be linearized for small angles θ with respect to an in-plane equilibrium magnetization. Solutions for this equation under for periodic driving are shown in Section 2.2. The corresponding experimental technique is ferromagnetic resonance (FMR), which measures the absorption of microwaves through the frequency-dependent susceptibility. FMR is the source of most data on the dynamical response of ferromagnetic materials and heterostructures. Experimental parameters, both in the "bulk" and possible modification through film surfaces (finite size effects) are reviewed in Section 2.3. Solutions for pulsed magnetization motion, relevant for the beginning or end of switching processes, are shown in Section 2.4.

2.1 LLG for thin-film, magnetized in plane, small angles

We will treat the magnetization dynamics of an ultrathin film, relevant for MRAM. Even for elements patterned to a 100 nm pillar, a 5 nm thick film ferromagnetic film can be approximated reasonably well as a

semi-infinite film. The magnetization is assumed to have its zero-field orientation in the yz plane. We take the film normal to be $\hat{\mathbf{x}}$. The magnetization is assumed to be saturated along $\hat{\mathbf{z}}$ in the presence of external applied fields along $\hat{\mathbf{z}}$, an approximation strictly true in limiting cases.[3].

Much of the interesting behavior in magnetization dynamics concerns only small excursions of the magnetization from its equilibrium direction. We introduce the following reduced variables (cgs omits μ_0) [17],

$$\omega_M \equiv \mu_0 \gamma M_s \qquad \omega_H \equiv \mu_0 \gamma H_z^{'} \qquad \lambda \equiv \mu_0 \gamma M_s \alpha \tag{19}$$

defining $H_z^{'} = H_B + H_K + \ldots$, an *effective field* including any uniaxial (or unidirectional) anisotropy fields maintaining the magnetization along the biased direction. (Surface anisotropy terms will be discussed later.) We can express Eq 10 in the form

$$\begin{bmatrix} \dot{m}_x \\ \dot{m}_y \end{bmatrix} = \begin{bmatrix} -\alpha\left(\omega_M + \omega_H\right) & -\omega_H \\ \omega_M + \omega_H & -\alpha\omega_H \end{bmatrix} \begin{bmatrix} m_x \\ m_y \end{bmatrix} + \begin{bmatrix} \alpha & 1 \\ -1 & \alpha \end{bmatrix} \begin{bmatrix} \gamma H_x^{eff} \\ \gamma H_y^{eff} \end{bmatrix}$$

under the assumption $m_x, m_y \ll 1$ and $m_z \simeq 1$.

Equation 2.1 is the most compact form of the LL equation, valid for small angles. This system of two coupled ordinary differential equations in m_x, m_y can be converted to a single second-order ordinary differential equation in m_y by differentiating the first and substituting the second into the first. After some algebra we can convert these equations into the classical equation for a driven harmonic oscillator,

$$\ddot{m}_y + \eta\, \dot{m}_y + \omega_0^2\, m_y = f_0^2 \cos\omega t \tag{20}$$

$$\eta = \alpha\left(\omega_M + 2\omega_H\right) \qquad \omega_0 = \sqrt{\omega_H\left(\omega_H + \omega_M\right)} \qquad f_0^2 \simeq \left(\omega_M + \omega_H\right)\gamma H_{y,0} \tag{21}$$

where the α term in the drive is neglected. A similar equation could be written for m_x. Note that all "constant" parameters, namely the the relaxation rate η, resonant frequency ω_0, and driving amplitude f_0, are functions of the applied field through ω_H.

Re-expanding the variables in SI units, we can write the *Kittel equation* for the resonant frequency of precession as

$$\nu_0 = \frac{\omega_0}{2\pi} = \frac{|\gamma_0|}{2\pi}\left(\frac{g_{eff}}{2}\right)\mu_0\sqrt{H_z'\left(H_z' + M_s\right)} \tag{22}$$

2.2 Ferromagnetic resonance

In their 1935 paper, Landau and Lifshitz worked through Eq. 6, derived a correct expression for $\chi(\omega)$ for a sphere, and predicted a large enhancement of microwave power absorption on resonance–all far before any experimental observation of magnetic resonance. Rabi and coworkers at Columbia reported the first experimental observation of NMR using time-of-flight techniques in 1938[18]. The observation of resonant absorption at microwave frequencies, relying on advances in radar technology[19], did not appear until 1945; the first observation of ESR[20] was followed rapidly by the first observation of NMR in 1946[21], then by FMR later that year[22]. The role of dipolar fields in increasing the in-plane resonance frequency for FMR (as $\gamma\sqrt{BH}$) was first understood by Kittel[23].

[3]Note that full alignment is strictly true only in the case of pure hard-axis or pure-easy axis alignment; see Section 2.

Microwave susceptibility The absorption of microwaves in an insulating ferromagnet is found through the imaginary susceptibility $\chi^{''}(\omega)$; eddy currents bring complications in conductive ferromagnets. From the equation for susceptibility in a forced harmonic oscillator, we can find $\chi(\omega)$ for the ferromagnetic thin film; neglecting terms in α^2

$$\chi_{M,\parallel} = \frac{M_y}{H_y} = \frac{M_s}{H_y}\frac{f_0^2}{(\omega_0^2-\omega^2)+i\eta\omega} = \frac{\omega_M\left(\omega_M+\omega_H\right)}{(\omega_0^2-\omega^2)+i\eta\omega} \tag{23}$$

which can be expressed in terms of reduced variables,

$$h \equiv \frac{\omega_H}{\omega_M} \qquad h \equiv \frac{H_z^{'}}{4\pi M_s} \qquad \Omega \equiv \frac{\omega}{\omega_M} \qquad \chi_M = \frac{h+1}{h\left(h+1\right)-\Omega^2+\left(1+2h\right)i\alpha\Omega} \tag{24}$$

On and near resonance, we can express $h = h_r + \Delta h$, where h_r is the field for resonance at fixed frequency Ω. We then have, neglecting terms $\Delta h^2 \ll 1$ and $\Delta h \ll h_r$,

$$\chi_M^{''} \simeq \alpha\Omega\frac{h_r+1}{(1+2h_r)}\frac{1}{(\Delta h)^2+\alpha^2\Omega^2}$$

We see that there is a Lorenzian (peaked) enhancement of imaginary susceptibility (power absorption) at the resonant frequency $\omega = \omega_0$, by a maximum of α^{-1}. Expressing the full-width in field for which $\chi^{''}$ reaches half its peak value, we have

$$\Delta H(\omega) = \Delta H_0 + \frac{2\alpha}{|\gamma|}\omega(cgs) \qquad \mu_0\Delta H(\omega) = \mu_0\Delta H_0 + \frac{2\alpha}{|\gamma|}\omega(SI) \tag{25}$$

to which we have added an inhomogeneous broadening term ΔH_0 due to large-scale magnetic disorder.

Extraction of materials parameters Equation 25 describes how to measure the damping α in a swept-field, variable frequency FMR experiment. The damping α is found through a linear fit to frequency-dependent linewidth $\Delta H(\omega)$, where α is given by the slope and ΔH_0 is given by the zero-frequency offset.[4] The range up to 70 Ghz is best for materials such as Fe. Measurements in the range 0-24 Ghz are most reliable where ferromagnetic materials are very soft and there is little contribution from magnetocrystalline anisotropy (e.g. $Ni_{81}Fe_{19}$.) The resonance position provides a good estimate of other materials parameters. From Eq we have $\omega_0 = \mu_0|\gamma|\sqrt{H_z^{'}\left(H_z^{'}+M_s\right)}$, so the slope of $\omega(H)$ becomes an effective measurement of M_s^{eff}, which contains the surface anisotropy; the offset provides a measure of H_K. For in-plane measurements, γ is best taken from tables.

Eddy currents Eq 25 cannot be used for the damping of thick metallic ferromagnetic films. Rado and Ament[25] have developed an expression for the equivalent permeability $\mu_{eff}(\omega)$ of semi-infinite films. The finite conductivity of the metal film implies a finite skin depth for microwaves; the skin depth is reduced compared with the nonmagnetic case by a factor $\mu_r^{-1/2}$. The inhomogeneous magnetization profile in the ferromagnet gives rise to inhomogeneous exchange fields, broadening the resonance. Experimental extraction of λ often failed in bulk whiskers[26] and oft-cited[27, 28] low-temperature values of λ for Co and Fe are in fact poorly known. Accurate measurements of α in ferromagnetic metals were enabled only through the production of ultrathin ferromagnetic films, where the Rado-Ament analysis was not necessary. For films

[4] An alternative view holds that disorder combined with exchange coupling between grains can also produce a frequency-dependent linewidth[24], but these complications are generally exhausted at relatively low frequencies (10-20 Ghz).

Material	g_{eff} (Ref [33, 34])	$\mu_0 M_s$ (T) (Ref [35])	$\alpha_0(\times 10^{-3})$	λ or G (Mhz)
Fe	2.094± 0.02	2.1545	1.8	57[36, 37, 38]
Co	2.170± 0.02	1.8173	8.5	170-280[37]
Ni	2.185± 0.02	0.6165	23.3	220[26]
$Ni_{81}Fe_{19}$ (Py)	2.129± 0.02 [2.09]	[0.95[39]-1.07[40]]	6.7	107
$Co_{60}Fe_{20}B_{20}$[40]	2.07	1.14	6.5[40]	107
$Co_{72}Fe_{18}B_{10}$[41]	2.07	1.76	6.0[40]	153

Table 1: Room-temperature values of materials parameters for several typical ferromagnets and ferromagnetic alloys. Precisions for g_{eff} are no better than 1%, for α and G, no better than 5%.

thinner than those which support a spin wave, Lock[29] has written an estimate for the damping due to eddy currents,

$$\lambda_{\text{eddy}} = |\gamma| M_s \alpha = \frac{\sigma}{12}(4\pi\gamma M_s)^2 \left(\frac{t}{c}\right)^2 (cgs) \qquad \lambda_{\text{eddy}} = |\gamma|\mu_0 M_s \alpha = \frac{\mu_0}{48\pi\rho}(\gamma\mu_0 M_s)^2\, t^2\ (SI) \tag{26}$$

where the $\lambda_{SI,cgs}$ values have been defined as equal previously. For Fe, with large M_s and small ρ, this can be substantially larger (by a factor of ∼8) than that of Py, forming a sizeable fraction of its bulk damping at 50 nm. Py is much less sensitive.[30] For films much thinner than the (magnetic) skin depth, eddy-current damping became insignificant, and it became possible to extract α directly from Eq 25 starting in the late 1960's[31]. The experimental program of B. Heinrich has centered on extraction of α in ultrathin epitaxial films[32, 3]

2.3 Tabulated materials parameters

The materials parameters which should be used in the LLG are reasonably well known in the bulk for elemental solids and "typical" soft alloys at room temperature. Finite size effects (thickness dependence) remain under investigation, particularly for the damping α. We show parameters for ferromagnetic metals in the "bulk" in Table 2.2. Tabulated dynamics parameters have been measured by FMR, which remains the most quantitative of magnetization dynamics techniques. Values of $\mu_0 M_s$ and g_{eff} come from magnetometry and are confirmed by magnetomechanical experiments, respectively.

2.3.1 Bulk values

Magnetic moments M_s were tabulated by Stearns in the Landolt-Bornstein tables[35], reprinted here at 300K.[5] The alloy values are less certain. For nominal $Ni_{81}Fe_{19}$ alloys, fits to FMR data have indicated a range of 0.95-1.07 T. Interpolation of the Ni, Fe values in Table 2.2 would yield an estimate of 0.91 T with a sensitivity to composition of 0.015T/%. For constant alloy sputtering target composition (nominal film composition), even though the exiting flux from the target is thought to converge to the internal composition, deposited compositions can vary, by up to 8% for e.g. the Ni-Ti system[42], due to differences in thermalization of the ejected atoms.

[5] For the elemental solids Fe, Co, Ni, the values given here for 300 K have been extrapolated from the 286.5 K values cited using factors of $1 - c\Delta T$ where $c_{Fe} = 1.2 \times 10^{-4} K^{-1}$, $c_{Co} = 5.9 \times 10^{-5} K^{-1}$, $c_{Ni} = -4.2 \times 10^{-4} K^{-1}$. Values are taken for Fe[110], Co[0001], Ni[111]; nonnegligible anisotropy in $\mu_0 M_s$ exists, to 0.5% in Co at zero temperature, on the order of 5×10^{-4} in the cubic solids.

Gyromagnetic ratios Gyromagnetic ratios are known from a combination of magnetomechanical measurements ($g^{'}$) and FMR measurements (g), taken on bulk samples, in some cases on the same bulk samples[33]; in careful experiments, good agreement (to better than 0.7% error) is found between the measurements satisfying the relationship $1/g^{'} + 1/g = 1$[43]. The error cited for each material is the error for the composition datapoint, typically <1%; fits to binary alloy series should improve the error. Later investigations confirmed these values[34]. Taking g_{eff} as a free parameter, allowed to range much outside of the band of values listed, or allowed to vary with thickness, is error-prone.

Damping The most structure-sensitive of the parameters is the damping α, but only in a particular sense. The values given here are α_0, the lowest values found in the literature for variable-frequency FMR spanning linewidth variations significantly greater than the inhomogeneous broadening; see Section 2.2. The Fe value of $\lambda/G = 57$ Mhz($\alpha = 0.0018$) is equal in sputtered films[37] and single-crystal whiskers[36] at room temperature in measurements up to 90 Ghz. Ni, also, shows $\lambda/G = 220$ Mhz($\alpha = 0.023$) equally in the two measurements[26]. Co has not been shown to fit the Rado-Ament analysis for whiskers. Measurements of nominally FCC films on MgO have shown different Gilbert damping parameters α for two different crystal directions, not expected for a cubic material.

A higher value of α_{eff} can be assumed for imperfect materials. However, α_{eff} is not expected to be constant with frequency: where damping is increased due to magnetic inhomogeneities (ΔH_0), effective $\alpha_{eff}(\omega)$ is a decreasing function of frequency, converging towards α_0; see Ref. [30]. ($\alpha \neq \alpha_0$ thus reflects some departure from a single-domain model.) Complicating the matter further is that the lowest values of α have been observed in sputtered films; crystallographically optimized MBE Fe films exhibit significantly higher values of α[44], attributed to the presence of vacancies[3].

2.3.2 Finite-size effects

Effective magnetization There is some question whether the bulk magnetization applies for ultrathin films. Where interface structure is well-controlled, it appears unlikely: experiments on epitaxial Co/Cu report, in roughly equal numbers, enhanced, reduced, or unchanged magnetic moment μ_B per Co interface *atom;* see Table 21 in [45]. In magnetization dynamics experiments, possible finite-size effects on magnetization are overwhelmed by *surface anisotropy*, proposed by Neél in the 1950's[46]. Surface anisotropy introduces free energy terms per unit area of the top and bottom FM interfaces as $U_{i,area} = -\sigma_i m_x^2$, where the interfaces favor in-plane magnetization for $\sigma < 0$. Thus

$$\mathbf{H_{eff}} = 2\frac{\sigma_{top} + \sigma_{bottom}}{\mu_0 M_s}\frac{1}{t_{FM}} m_x \hat{\mathbf{x}} \qquad \mu_0 M_s^{eff} = \mu_0 M_s - \frac{4\sigma}{M_s}\frac{1}{t_{FM}} \tag{27}$$

which, as can be seen, has the sole effect of changing the "effective" $\mu_0 M_s$ resulting from a fit of the form Eq 22. First identifications of surface anisotropy in FMR experiments date from the 1970s, though film preparation is in question for experiments from this era. Py/air was identified to have a surface anisotropy of σ =0.08 mJ/m^2.[47] More recently, Rantschler et al have estimated σ in Py/Cu, Py/Ag, Py/Ta, finding 0.100, 0.100, and 0.070 mJ/m^2, respectively[48]. The positive surface anisotropy, which favors perpendicular magnetization, has the effect of *reducing* the resonance frequencies as if $\mu_0 M_s$ were reduced. In a Cu/Py(5 nm)/Cu film, $\mu_0 M_s^{eff}$ becomes reduced by roughly 0.1 T.

Gyromagnetic ratio It is not clear whether there is a size effect in the gyromagnetic ratio. Some have proposed that the balance μ_L/μ_S could be enhanced in structures of finite dimension[49], making larger values of g_{eff} plausible in ultrathin films. Variable-frequency, perpendicular FMR (normal condition) is

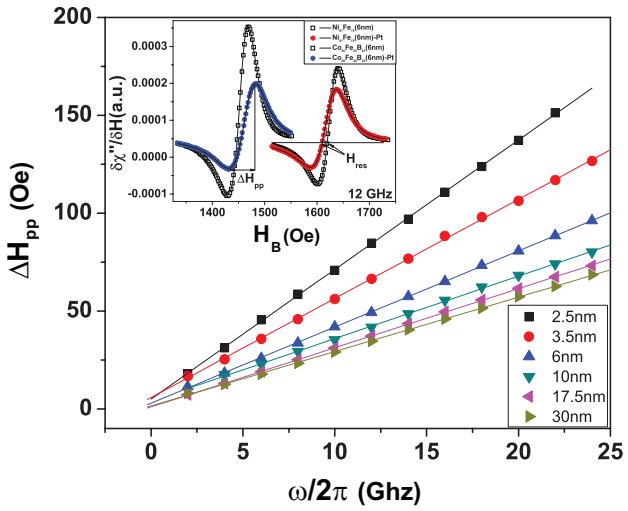

Figure 1: Illustration of damping size effect: FMR linewidth ΔH_{pp} as a function of frequency $\omega/2\pi$ for $Ni_{81}Fe_{19}(t_{FM})$ with Cu(3nm)/Pt(3nm) overlayers. There is an inverse dependence of α on the t_{FM} as shown in the slope of the curve. *Inset:* experimental trace of absorption derivative $\partial\chi^{''}/\partial H$

best suited to determine g_{eff} since it enables its isolation from the slope $\Delta H_{res}/\Delta\omega$. Identifications of a size effect[50, 51] in g_{eff} have relied on in-plane FMR or PIMM, where (at low frequency) $\nu^2 \propto g_{eff}^2 M_s^{eff}$; values of g_{eff} as high as 2.6 were extracted for the Co(3nm)/Cu system, but with $\mu_0 M_s$ correspondingly lower than given in Table 2.2.

Damping α There is good evidence that the damping α itself exhibits a size effect, where $\alpha = \alpha_0 + Kt^n$. In structures with "spin sinks" in proximity to the FM layer, either heavy elements such as Pt or other FM layers, *spin pumping* can increase α by a factor of roughly two over bulk values at thicknesses between 2-5 nm, with inverse dependence on FM thickness ($n = -1$). A detailed review of experiments and theory to 2005 was given by Tserkovnyak[52]. However, even in structures without a spin sink layer, a similar size effect in damping is present. The origin of this size effect is not known.

2.4 Pulsed magnetization dynamics

Equation 20, derived under the assumption of small amplitudes, $\alpha \ll 1$, and sinusoidal driving fields, can be rewritten for arbitrary transverse external fields $H_y(t)$

$$\ddot{m}_y + \eta\,\dot{m}_y + \omega_0^2\, m_y = (\omega_M + \omega_H)\,\mu_0\gamma H_y(t) \tag{28}$$

where the longitudinal field $\omega_H = |\gamma|\mu_0 H_{B,Z}^{'}$ is taken to be constant. For a step function in transverse magnetic field, the magnetization trajectory describes a damped sinusoid with initial conditions dependent on the initial state. The simplest case is where a finite rotation, in-plane angle $\theta_0 \simeq m_{y0} = m_y(t = 0)$, relaxes to zero after removal of a finite-width, fast fall-time pulse (falling step). The solution for Eq 28 is

$$m_y(0) = e^{-t/\tau}\cos\omega_0 t \qquad \tau = \frac{2}{\eta} \tag{29}$$

where η, ω – both field-dependent– are given as in Eq. 21. It is less straightforward to incorporate inhomogeneous broadening in this expression; one can calculate a frequency linewidth by multiplying $\Delta H(\omega)$ by $\partial\omega_0/\partial H$, which can be substituted in the expression for η.

The first high-speed inductive measurements of magnetization dynamics were carried out at IBM-Zurich in the early 1960s[53]; the 350 ps risetime of the pulse was sufficient to look at low-frequency precessional dynamics ($\sim$ 1 Ghz). The NIST-Boulder group updated the technique using electronics with higher frequency capability[54], and have investigated precessional dynamics up to 3 Ghz[55]. Pump-probe magnetooptical Kerr effect measurements of small angle magnetization dynamics, demonstrated first on EuS films[56], were extended to metallic ferromagnetic systems[8], also by the NIST group. Similar experiments have been carried out on lithographically defined micron-size structures, monitored through time-dependent magnetoresistance.[57]

3 Large-angle dynamics: switching

In this section, we consider the limit of motions up to 180°. In Section 3.1, we develop a model for the quasistatic switching of a single domain with arbitrary in-plane anisotropy axis. We show that there is a critical field large enough for spontaneous switching at any temperature, with an energy barrier for lower fields. In Section 3.2, we develop a simple model for thermal reversal rates over the barrier. Thermally activated switching is relevant for the small patterned elements used in MRAM and essential in some switching schemes. Finally, in Section 3.3, we show integrated switching trajectories for single-domain thin film elements, illustrating the effect of damping α.

3.1 Quasistatic limit: Stoner-Wolfarth model

In this section, we will consider the quasistatic switching behavior of a single-domain magnetic particle with well-defined ansiotropy. Note that any behavior described here can be described, in greater detail, through direct integration of the LLG. The LLG reaches equilibrium $\dot{\mathbf{m}} = 0$ where the precessional term is zero. Thus the torque

$$\tau = \mathbf{m} \times \mathbf{H_{eff}} = 0 \tag{30}$$

or, equivalently, magnetization $\mathbf{m}$ and applied effective fields $\mathbf{H_{eff}}$ are collinear. This is a useful property in simulation: micromagnetic ground states (for N particles coupled through magnetostatics or otherwise) can be found by integrating the LLG forward to convergence, accelerated by taking unphysically large values of α.

Energy expression We assume that the particle has some "built-in" structure, or *anisotropy* which favors magnetization in a particular direction. This model was first considered by Stoner and Wohlfarth in 1948[58]. The anisotropy can be expressed as a contribution to the energy U_A which depends on the magnetization orientation ϕ,

$$U_A(\phi) = K_u \sin^2(\phi - \phi_u) \tag{31}$$

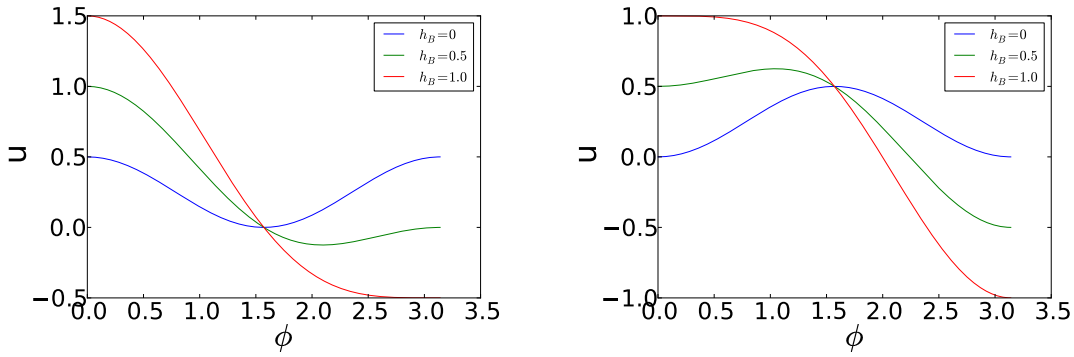

Figure 2: Energy landscapes, hard axis (left) and easy axis (right.) Note the metastable equilibria at $\theta = \pi$ for the easy-axis case if $h_B < 1$.

where ϕ_u is the angle of the preferred direction of the magnetization. The energy is *minimized* where $\phi = \phi_u$ and *maximized* where $\phi = \phi_u \pm \pi/2$ ("hard axis"), but is equivalent for $\phi = \phi_u$ and $\phi = \phi_u \pm \pi$ ("easy axis"). The anisotropy axis thus has no direction, only an orientation. K_U is an anisotropy constant and takes units of erg/cm^3.

Defining

$$H_K \equiv \frac{2K_u}{M_s} \qquad h_B = \frac{H_B}{H_K} \qquad u = \frac{U}{M_s H_K} \tag{32}$$

the normalized total energy including Zeeman and anisotropy terms is

$$u = -m_z h_B + \frac{1}{4}\left[1 - \cos 2\phi \cos 2\phi_u + \sin 2\phi \sin 2\phi_u\right] \tag{33}$$

Hard and easy axis magnetization In the hard axis case, $\phi_u = \pi/2$; in the easy-axis case, $\phi_u = 0$. For these two cases, Eq. 33 becomes

$$u_{HA} = -m_z h_B + \frac{1}{2} m_z^2 \qquad u_{EA} = -m_z h_B + \frac{1}{2}\left(1 - m_z^2\right) \tag{34}$$

since $m_z = \cos\phi$. We can find the equilibrium magnetization by taking the first derivative of u with respect to m_z, and find

$$m_z^{HA} = h_B \qquad m_z^{EA} = -h_B \tag{35}$$

which is a stable minimum only for the hard axis case. The energy minimum for the easy axis case must lie on either extremum, $\phi = 0$ or $\phi = \pi$. Clearly the lowest energy is found for $\phi = 0$ for $h_z > 0$ and $\phi = \pi$ for $h_z < 0$.

Switching does not respond simply to the energy minimum. For an initial state $\phi = \pi$ under the application of $0 < h_z < 1$, or $H_B < H_K$, the $\phi = 0$ state becomes lower and lower in energy compared with

the $\phi = \pi$ state, but the single domain cannot rotate into it. As illustrated in Figure 2, an energy barrier develops between the two states. Small excursions away from $\phi = \pi$ only raise the energy. Only when the $du/d\phi < 0$ over the whole domain $-1 < h_B < 1$ will the particle switch. This condition becomes true for $h_B \geq 1$ or $H_B > H_K$. For lower fields, thermal activation is required to mount the energy barrier.

General case: the switching asterøid Richer behavior emerges if we consider the problem more generally. We would like to consider the critical field for switching h_0. We now allow both the reduced magnetization $\mathbf{m} = \mathbf{M}/M_s$ and the reduced field $\mathbf{h} = \mathbf{H}/H_K$ to take any direction in the xy plane. We will see that the critical field is a function of angle as well as magnitude, so $\mathbf{h_0}$ is a dividing line in the control plane. This geometrical approach originates with Slonczewski. Here we follow Thiaville's notation[59]. A convenient aspect of this formulation is that it can be used for any form of the in-plane anisotropy energy, given here as $G(\phi)$. The magnetization takes angle ϕ with respect to the x-axis, giving us magnetization vector $\mathbf{m}$ and its orthogonal in-plane vector $\hat{\mathbf{e}} \equiv \hat{\phi}$; this is a different coordinate system than the yz film plane considered up until now.

$$\mathbf{m}(\phi) = \cos\phi\,\hat{\mathbf{x}} + \sin\phi\,\hat{\mathbf{y}} \qquad \hat{\phi} = \mathbf{e} = -\sin\phi\,\hat{\mathbf{x}} + \cos\phi\,\hat{\mathbf{y}} \tag{36}$$

$$\frac{\partial \mathbf{m}(\phi)}{\partial \phi} = \mathbf{e} \qquad \frac{\partial^2 \mathbf{m}(\phi)}{\partial \phi^2} = -\mathbf{m} \tag{37}$$

To find equilibria, we already know to take

$$\frac{\partial}{\partial \phi}\left(-\mathbf{m}(\phi)\cdot\mathbf{h_0} + u_A(\phi)\right) = -\mathbf{e}\cdot\mathbf{h_0} + \frac{\partial u_A(\phi)}{\partial \phi} = 0 \tag{38}$$

and for stability, $\partial^2 u/\partial\phi^2 = 0$.

$$\frac{\partial}{\partial \phi}\left(-\mathbf{e}\cdot\mathbf{h_0} + \frac{\partial u_A(\phi)}{\partial \phi}\right) = \mathbf{m}\cdot\mathbf{h_0} + \frac{\partial^2 u_A(\phi)}{\partial \phi^2} = 0 \tag{39}$$

Decomposing $\mathbf{h_0} = h_0^m\,\mathbf{m} + h_0^e\,\mathbf{e}$, these two criteria give

$$\mathbf{h_0} = -\frac{\partial^2 u_A(\phi)}{\partial \phi^2}\,\mathbf{m} + \frac{\partial u_A(\phi)}{\partial \phi}\,\mathbf{e} = -G''\,\mathbf{m} + G'\,\mathbf{e} \tag{40}$$

From here, we can transfer back into the Cartesian system using Equations 36 and 37

$$\mathbf{h_0} = -\left(G''\cos\phi + G'\sin\phi\right)\,\hat{\mathbf{x}} + \left(-G''\sin\phi + G'\cos\phi\right)\,\hat{\mathbf{y}} \tag{41}$$

Fixing $\hat{\mathbf{x}}$ for the uniaxial anisotropy easy axis, after some algebra, yields

$$\mathbf{h_0} = -\cos^3\phi\,\hat{\mathbf{x}} + \sin^3\phi\,\hat{\mathbf{y}} \tag{42}$$

For $\phi = 0$ ($m = 1$) and $\phi = \pi$ ($m = -1$) , the magnetization lies along the easy axis. In order to destabilize the positive (negative) magnetization $m = \pm 1$, it is necessary to apply an opposite, negative (positive) field $H = \mp H_k$, or $h = \mp 1$. The boundary between switching and no switching, known as the *switching astrøid*, is shown in Figure 3.

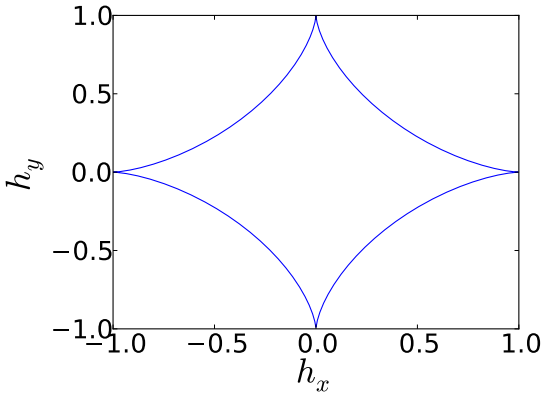

Figure 3: The switching astroid described by Eq. 42. Magnetization does not become destabilized until the field $|h|$ lies outside the boundary.

3.2 Thermal switching

For easy-axis switching, we saw that for applied fields large enough, $h > -m$, there is no energy barrier for reversal. Magnetization reversal is continuously energetically favored for rotation of ϕ away from $\phi = 0$. For smaller, subcritical fields $|h| < 1$ directed along the easy axis, an energy barrier exists for switching, as shown in Fig 2. If no thermal energy were available, a particle would never switch for $|h| < 1$. Thermal fluctuations help drive the magnetization over the barrier, and yield a finite, thermally activated switching rate which depends on the applied field and volume of the particle.

In Eq. 34, if we take our starting point as $m_z = 1$ ($\phi = 0$) and apply a field h along $-\hat{\mathbf{z}}$ (opposite to the magnetization direction), we find that the energy difference between the initial state and the unstable equilibrium at $m_z = -h$ is

$$\Delta u = u_{eq} - u(\phi = 0) \qquad \Delta u = \frac{1}{2}\left(1 - h_B\right)^2 \tag{43}$$

The Arrhenius-Neel equation for kinetics (e.g. Ref [60]) states that the frequency ν of overcoming the barrier (and switching) should be

$$\nu(\Delta U, V, T) = \nu_0\, e^{-\Delta E_b/k_B T} \qquad \Delta E_b = \frac{1}{2} M_s H_K V \left(1 - \frac{H_B}{H_K}\right)^n \qquad n = 2 \tag{44}$$

for an energy barrier ΔE_b. k_B is the Boltzmann constant, $k_B(300\text{K}) = 25.86$ meV, ν_0 is a temperature-independent "attempt frequency." The value $n = 2$ obtains for easy-axis switching; for the full Stoner-Wolfarth model with arbitrary orientation of the anisotropy axes (not shown here), $1.5 \leq n \leq 2$. Expressing a characteristic time $\tau = \nu^{-1}$, if a switching experiment is carried out many times, the number of times N the particle does *not* reverse in time t is given by

$$\frac{\partial N}{\partial t} = -\frac{N}{\tau} \qquad N(t) = N_0\, e^{-t/\tau} \tag{45}$$

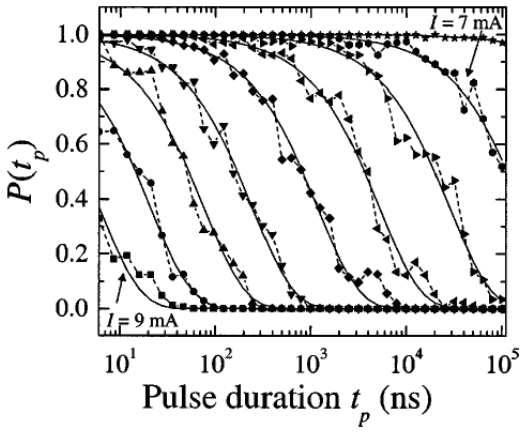

Figure 4: Probability of not-switching of a magnetic tunnel junction in response to field pulses of width t_p, $P_{ns}(t_p)$, variable pulse amplitude i. From Ref [62].

for N_0 attempts. The probability for switching after time t $P_s(t)$ is thus

$$P_s(t) = 1 - P_{ns}(t) = 1 - e^{-t/\tau} \qquad \tau = \nu_0^{-1} e^{\Delta E_b / k_B T} \tag{46}$$

where ΔE_b was given in Eq 44. Wernsdorfer and coworkers[61] applied Eq 46 to the low-temperature (0.2-6 K) and low-speed switching of a single 25 nm diameter Co nanoparticle, measured through a SQUID microbridge with temporal resolution of ~ 250 μs.

Thermal switching experiments: MRAM In the context of MRAM, Rizzo and coworkers at Motorola applied Eq. 46, $n = 2$, to the thermal switching in magnetic tunnel junctions[62] for pulse durations t_p of 5ns-100μs at room temperature. The magnetic state was characterized through the magnetoresistance. Data are shown in Figure 4 for the probability of not-switching after pulse duration t_p $P_{ns}(t_p)$ under the application of field pulses with different values (currents) of H/H_K (given there as i/i_{sw}). Excellent agreement is shown with the single-domain / single-energy-barrier model. Other contemporaneous experiments showed more complicated behavior, with multiple energy barriers indicating thermal activation of domain walls[63]. Further experiments characterized the full thermal switching astrøid, with arbitrary pulse direction, at constant sweep rate[64].

3.3 Switching trajectory

In this section we will examine a calculated trajectory for switching of a thin-film element. A convenient dimensionless form can be used for integration if we take out a factor $T = \mu_0 \gamma M_s$. Defining dimensionless $t' = T \cdot t$,

$$T^{-1} \begin{bmatrix} \dot{\theta} \\ \dot{\phi} \end{bmatrix} = \begin{bmatrix} \partial\theta/\partial t' \\ \partial\phi/\partial t' \end{bmatrix} = \frac{1}{1+\alpha^2} \begin{bmatrix} \alpha & 1 \\ -1/\sin\theta & \alpha/\sin\theta \end{bmatrix} \begin{bmatrix} h_\theta^{eff} \\ h_\phi^{eff} \end{bmatrix} \tag{47}$$

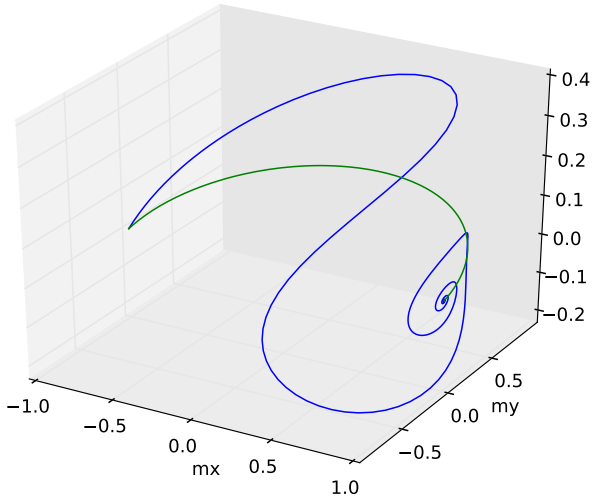

Figure 5: Switching on the unit sphere (phase plot, implicit in time), under the influence of $h = +1$, initial condition $m_x = -1$, thin film magnetized in (xy) film plane. The z-axis is taken to be the film normal. Trajectories for $\alpha = 1$ and $\alpha = 0.1$ are shown. Total integration time is $t^{'} = 100$, or ∼6 ns.

Note that for Py, for example, $t^{'} = 1$ is reached for $t = 64.5$ ps. Fields can be transferred from the rotating frame to the cartesian frame through

$$\begin{bmatrix} h_\theta \\ h_\phi \end{bmatrix} = \begin{bmatrix} \cos\theta\cos\phi & \cos\theta\sin\phi & -\sin\theta \\ -\sin\phi & \cos\phi & 0 \end{bmatrix} \begin{bmatrix} h_x \\ h_y \\ h_z \end{bmatrix} \tag{48}$$

Example: influence of α For a useful example, we can take a thin film magnetized in plane, evolving under the influence of an in-plane switching field. To be consistent with the form where the polar axis is $\hat{\mathbf{z}}$, the film plane is xy, and we have effective fields as follows:

$$h_x = h_b \qquad h_z = -\cos\theta \tag{49}$$

$$\begin{bmatrix} h_\theta \\ h_\phi \end{bmatrix} = \begin{bmatrix} h_b\cos\theta\cos\phi + \sin\theta\cos\theta \\ -h_b\sin\phi \end{bmatrix} \tag{50}$$

The expression for direct integration is then given as

$$\begin{bmatrix} \partial\theta/\partial t^{'} \\ \partial\phi/\partial t^{'} \end{bmatrix} = \frac{1}{1+\alpha^2} \begin{bmatrix} \alpha & 1 \\ -1/\sin\theta & \alpha/\sin\theta \end{bmatrix} \begin{bmatrix} h_b\cos\theta\cos\phi + \sin\theta\cos\theta \\ -h_b\sin\phi \end{bmatrix} \tag{51}$$

We show integrated trajectories from $m_x = -1$ to $m_x = +1$ in Figure 5. Notice the influence of α on the convergence towards a new equilibrium direction, very rapid for $\alpha = 1$, and less direct for $\alpha = 0.1$. The effective field from demagnetization keeps the magnetization trajectory more in-plane than out of plane.

4 Magnetization switching by spin-transfer

In this final section, we show how spin torque terms are added to the LLG equation (Section 4.1), write the full LLG with spin torque terms (Section 4.2), and show a simple estimate for the SMT switching current. Sun has presented a thorough set of calculations of spin-torque switching for single domains, with anisotropy and thermal activation, in [65].

4.1 Additional terms to the LLG

Spin polarized currents can act as an additional source for torque on the magnetization[66][67]. A spin-polarized electron carries an angular momentum $\hbar$. If the electron is scattered in the FM layer, reversing its spin through transfer of angular momentum to $\mathbf{m}$, $\mathbf{m}$ rotates according to the torque exerted. This is *spin transfer torque*. The angular momentum transferred per unit time (torque) is thus $\tau \sim 2\hbar JSP/e$, where J is the current density, e is the electronic charge, $0 < P < 1$ is the spin polarization, and S is the area. Taking $\hat{\mathbf{p}}$ as the *spin* direction of the spin polarized current incident on the FM[6], we have for the additional term to magnetization dynamics, through Eq. 13

$$\tau = -\frac{|\gamma|}{St\mu_0 M_s}\tau(SI) \qquad \dot{\mathbf{m}}_{STT} = -\frac{2\hbar J|\gamma|P}{e\mu_0 M_s t}\hat{\mathbf{p}} \tag{52}$$

Most interesting to note here is that there can only be a contribution to magnetization dynamics where $\mathbf{m}$ and $\mathbf{p}$ form angles other than zero and π. Any components of $\dot{\mathbf{m}}_{STT}$ which are parallel to $\mathbf{m}$ will make no contribution, since torque terms can only rotate the magnetization, $\dot{\mathbf{m}} \cdot \mathbf{m} = 0$. The transverse component of the spin current can be isolated by taking $\mathbf{M} \times \mathbf{M} \times \hat{\mathbf{p}}$ and the contribution to magnetization dynamcs given by spin torque is

$$\dot{\mathbf{m}} = \ldots + \gamma A_J \mathbf{m} \times \mathbf{m} \times \mathbf{p} + \gamma B_J \mathbf{m} \times \mathbf{p} \qquad A_J \equiv AJ \simeq \frac{2\hbar}{e} P \frac{1}{\mu_0 M_s}\frac{1}{t} J \tag{53}$$

where A_J is the *Slonczewski* spin torque. A_J is an experimental parameter, proportional to (an odd function of) current density J, with estimate as given. B_J is the *field-like* spin torque, introduced separately; its dependence on current and voltage is under investigation.[68, 69] Both terms have units of field (T).

4.2 Full-angle LLG with spin-torque

In terms of the magnetization coordinates, Eq 52 can be expressed

$$\dot{\mathbf{m}} = \ldots + \gamma A_J \hat{\mathbf{m}} \times \hat{\mathbf{m}} \times \left(p_\theta \hat{\theta} + p_\phi \hat{\phi}\right) + \gamma B_J \hat{\mathbf{m}} \times \left(p_\theta \hat{\theta} + p_\phi \hat{\phi}\right) \tag{54}$$

Defining $T = \gamma\mu_0 M_s$, normalized time $t' = T \cdot t$ and normalized spin torque parameters $A'_J = A_J/M_s$, $B'_J = B_J/M_s$, the single-particle, full angle LLG with spin torque can be written

[6] i.e. the direction of $\mathbf{m_2}$ if current is injected from $\mathbf{m_2}$ into $\mathbf{m_1}$

$$T^{-1}\begin{bmatrix}\dot{\theta}\\ \dot{\phi}\end{bmatrix} = \frac{1}{1+\alpha^2}\begin{bmatrix}\alpha & 1\\ -1/\sin\theta & \alpha/\sin\theta\end{bmatrix}\begin{bmatrix}h_\theta^{eff}\\ h_\phi^{eff}\end{bmatrix} \tag{55}$$

$$+\frac{1}{1+\alpha^2}\begin{bmatrix}-A'_J-\alpha B'_J & \alpha A'_J - B'_J\\ (B'_J-\alpha A'_J)/\sin\theta & (-A'_J-\alpha B'_J)/\sin\theta\end{bmatrix}\begin{bmatrix}p_\theta\\ p_\phi\end{bmatrix} \tag{56}$$

Nulling of damping If the effective field and the injected spin polarization, $\mathbf{H}$ and $\hat{\mathbf{p}}$, are collinear, the effective damping can be made zero through the spin torque. Damping is expressed in the on-diagonal terms of the right-hand-side of the equation. These cancel in the case of

$$A_J \geq \alpha H \tag{57}$$

Since it is known that A_J is proportional to current, we can express

$$A_J = A\,J \geq \alpha H \qquad J \geq \frac{\alpha H}{A} \tag{58}$$

Zero damping implies that equilibrium magnetization becomes unstable to any perturbation. A remarkable result of the nonlinear aspects of the LLG is that a limit cycle, oscillating around the equilibrium, can replace the stable state. The stable precession is the basis of the spin torque oscillator, a microwave power source driven by dc currents.

For higher values of current density J, the limit cycle becomes destabilized, replaced by stable equilibrium π away. This is *spin-torque switching*. Equation 58 suggests that lower-current (lower-power) spin-torque switching is favored by materials with lower values of damping α.

References

[1] M. Farle, "Ferromagnetic resonance of ultrathin metallic layers," *Reports on Progress in Physics*, vol. 61, p. 755, 1998.

[2] S. Russek, R. McMichael, M. Donahue, and S. Kaka, *Spin Dynamics in Confined Magnetic Structures II*.

[3] B. Heinrich, *Ultrathin magnetic structures: fundamentals of nanomagnetism*, vol. III, ch. 5, pp. 143–210. Springer, 2005.

[4] D. Ralph and M. Stiles, "Spin transfer torques," *Journal of Magnetism and Magnetic Materials*, vol. 320, no. 7, pp. 1190 – 1216, 2008.

[5] I. Mayergoyz, G. Bertotti, and C. Serpico, *Nonlinear magnetization dynamics in nanosystems*. Elsevier Science, 2008.

[6] L. Landau and E. Lifshits, "On the theory of the dispersion of magnetic permeability in ferromagnetic bodies," *Phys. Zeitsch. der Sow.*, vol. 8, pp. 153–69, 1935. Reprinted and translated as [70].

[7] H. Brooks, "Ferromagnetic anisotropy and the itinerant electron model," *Phys. Rev.*, vol. 58, pp. 909–918, Nov 1940.

[8] T. Crawford, T. Silva, C. Teplin, and C. Rogers, "Subnanosecond magnetization dynamics measured by the second-harmonic magneto-optic kerr effect," *Applied Physics Letters*, vol. 74, pp. 3386–8, May 1999.

[9] R. Liboff, *Introduction to Quantum Mechanics*. Addison-Wesley, 4 ed., 2002.

[10] A. Einstein and W. De Haas, "Experimental proof of ampere's molecular currents," *Verhandlungen der Deutschen Physikalischen Gesellschaft*, vol. 17, no. 8, pp. 152 – 170, 1915.

[11] V. Y. Frenkel, "On the history of the einstein-de haas effect," *Sov. Phys. Usp.*, vol. 22, pp. 580–4, July 1979.

[12] S. J. Barnett, "Magnetization by rotation," *Phys. Rev.*, vol. 6, pp. 239–270, Oct 1915.

[13] S. Barnett and G. Kenny, "Gyromagnetic ratios of iron, cobalt and many binary alloys of iron, cobalt and nickel," *Physical Review*, vol. 87, pp. 723 – 734, 1 Sept. 1952.

[14] T. Gilbert, "A lagrangian formulation of the gyromagnetic equation of the magnetic field," *Physical Review*, vol. 100, p. 1243, 1955. (abstract only).

[15] T. Gilbert, "A phenomenological theory of damping in ferromagnetic materials," *IEEE Transactions on Magnetics*, vol. 40, no. 6, pp. 3443 – 9, 2004.

[16] W. Saslow, "Landau-lifshitz or gilbert damping? that is the question," *Journal of Applied Physics*, vol. 105, no. 7, pp. 07 – 315, 2009.

[17] N. Chan, V. Kambersky, and D. Fraitova, "Impedance matrix of thin metallic ferromagnetic films and SSWR in parallel configuration," *Journal of Magnetism and Magnetic Materials*, vol. 214, no. 1-2, pp. 93 – 8, 2000.

[18] I. I. Rabi, J. R. Zacharias, S. Millman, and P. Kusch, "A new method of measuring nuclear magnetic moment," *Phys. Rev.*, Feb 1938.

[19] P. Forman, "Swords into ploughshares: Breaking new ground with radar hardware and technique in physical research after world war ii," *Rev. Mod. Phys.*, vol. 67, pp. 397–455, Apr 1995.

[20] E. Zavoisky, "Paramagnetic relaxation of liquid solutions for perpendicular fields," *J. Phys USSR*, vol. 9, pp. 211–6, 1945.

[21] E. M. Purcell, H. C. Torrey, and R. V. Pound, "Resonance absorption by nuclear magnetic moments in a solid," *Phys. Rev.*, vol. 69, pp. 37–38, Jan 1946.

[22] J. Griffiths, "Anomalous high-frequency resistance in ferromagnetic metals," *Nature*, vol. 158, p. 670, Nov 1946.

[23] C. Kittel, "Interpretation of anomalous larmor frequencies in ferromagnetic resonance experiment," *Phys. Rev.*, vol. 71, pp. 270–271, Feb 1947.

[24] R. McMichael and P. Krivosik, "Classical model of extrinsic ferromagnetic resonance linewidth in ultrathin films," *IEEE Transactions on Magnetics*, vol. 40, no. 1, pp. 2 – 11, 2004.

[25] W. Ament and G. Rado, "Electromagnetic effects of spin wave resonance in ferromagnetic metals," *Physical Review*, vol. 97, no. 6, pp. 1558–66, 1955.

[26] S. Bhagat and P. Lubitz, "Temperature dependence of ferromagnetic relaxation in the 3d transition metals," *Physical Review B (Condensed Matter)*, vol. 10, pp. 179–85, 1974.

[27] K. Gilmore, Y. U. Idzerda, and M. D. Stiles, "Identification of the dominant precession-damping mechanism in Fe, Co, and Ni by first-principles calculations," *Physical Review Letters*, vol. 99, no. 2, p. 027204, 2007.

[28] M. Fähnle, J. Seib, and C. Illg, "Relating Gilbert damping and ultrafast laser-induced demagnetization," *Physical Review B*, vol. 82, no. 14, pp. 144405 (4 pp.) –, 2010.

[29] J. Lock, "Eddy current damping in thin metallic ferromagnetic films," *British Journal of Applied Physics*, vol. 17, pp. 1645–7, 1966.

[30] C. Scheck, L. Cheng, and W. Bailey, "Low damping in epitaxial sputtered Fe films," *Applied Physics Letters*, vol. 88, no. 18, p. 252510, 2006.

[31] C. Patton, "Linewidth and relaxation processes for the main resonance in the spin-wave spectra of ni-fe alloy films," *Journal of Applied Physics*, vol. 39, no. 7, pp. 3060–8, 1968.

[32] B. Heinrich, K. Urquhart, A. Arrott, J. Cochran, K. Myrtle, and S. Purcell, "Ferromagnetic-resonance study of ultrathin bcc fe(100) films grown epitaxially on fcc ag(100) substrates," *Physical Review Letters*, vol. 59, no. 15, pp. 1756 – 9, 1987.

[33] A. Meyer and G. Asch, "Experimental g' and g values of fe, co, ni and their alloys," *Journal of Applied Physics*, vol. 32, no. 3, pp. 330 – 333, 1961.

[34] R. A. Reck and D. L. Fry, "Orbital and spin magnetization in fe-co, fe-ni, and ni-co," *Phys. Rev.*, vol. 184, pp. 492–495, Aug 1969.

[35] *Landolt-Bornstein Tables*, ch. III-13: Metals: Phonon States, Electron States, and Fermi Surfaces, pp. 100–101. Springer Verlag, 1990.

[36] Z. Frait and D. Fraitova, "Ferromagnetic resonance and surface anisotropy in iron single crystals," *Journal of Magnetism and Magnetic Materials*, vol. 15-18, no. pt.2, pp. 1081 – 2, 1980.

[37] "Gilbert damping and g-factor in Fe_xCo_{1-x} alloy films," *Solid State Communications*, vol. 93, no. 12, pp. 965 – 968, 1995.

[38] C. Scheck, L. Cheng, I. Barsukov, Z. Frait, and W. Bailey, "Low relaxation rate in epitaxial vanadium-doped ultrathin iron films," *Physical Review Letters*, vol. 98, no. 11, pp. 117601 – 1, 2007.

[39] Y. Guan and W. Bailey, "Ferromagnetic relaxation in $(ni_{81}fe_{19})_{1-x}cu_x$ thin films: band filling at high z," *Journal of Applied Physics*, vol. 101, no. 09, p. D104, 2007.

[40] A. Ghosh, J. F. Sierra, S. Auffret, U. Ebels, and W. E. Bailey, "Dependence of nonlocal Gilbert damping on the ferromagnetic layer type in ferromagnet/Cu/Pt heterostructures," *Applied Physics Letters*, vol. 98, no. 5, p. 052508, 2011.

[41] C. Bilzer, T. Devolder, J.-V. Kim, G. Counil, C. Chappert, S. Cardoso, and P. P. Freitas, "Study of the dynamic magnetic properties of soft cofeb films," *Journal of Applied Physics*, vol. 100, no. 5, p. 053903, 2006.

[42] M. Bendahan, P. Canet, J.-L. Seguin, and H. Carchano, "Control composition study of sputtered ni?ti shape memory alloy film," *Materials Science and Engineering: B*, vol. 34, no. 2-3, pp. 112 – 115, 1995.

[43] C. Kittel, "On the gyromagnetic ratio and spectroscopic splitting factor of ferromagnetic substances," *Phys. Rev.*, vol. 76, pp. 743–748, Sep 1949.

[44] R. Urban, G. Woltersdorf, and B. Heinrich, "Gilbert damping in single and multilayer ultrathin films: role of interfaces in nonlocal spin dynamics," *Physical Review Letters*, vol. 87, pp. 217204–7, 2001.

[45] C. A. F. Vaz, J. A. C. Bland, and G. Lauhoff, "Magnetism in ultrathin film structures," *Reports on Progress in Physics*, vol. 71, no. 5, p. 056501, 2008.

[46] Néel, Louis, "Anisotropie magnétique superficielle et surstructures d'orientation," *J. Phys. Radium*, vol. 15, no. 4, pp. 225–239, 1954.

[47] G. C. Bailey and C. Vittoria, "Presence of magnetic surface anisotropy in permalloy films," *Phys. Rev. B*, vol. 8, pp. 3247–3251, Oct 1973.

[48] J. O. Rantschler, P. J. Chen, A. S. Arrott, R. D. McMichael, J. W. F. Egelhoff, and B. B. Maranville, "Surface anisotropy of permalloy in NM/NiFe/NM multilayers," *Journal of Applied Physics*, vol. 97, no. 10, p. 10J113, 2005.

[49] P. Gambardella, S. Rusponi, M. Veronese, S. S. Dhesi, C. Grazioli, A. Dallmeyer, I. Cabria, R. Zeller, P. H. Dederichs, K. Kern, C. Carbone, and H. Brune, "Giant magnetic anisotropy of single cobalt atoms and nanoparticles," vol. 300, no. 5622, pp. 1130–1133, 2003.

[50] J. P. Nibarger, R. Lopusnik, Z. Celinski, and T. J. Silva, "Variation of magnetization and the Landé g factor with thickness in Ni-Fe films," *Applied Physics Letters*, vol. 83, no. 1, pp. 93–95, 2003.

[51] J.-M. Beaujour, J. Lee, A. Kent, K. Krycka, and C.-C. Kao, "Magnetization damping in ultrathin polycrystalline Co films: evidence for nonlocal effects," *Physical Review B (Condensed Matter and Materials Physics)*, vol. 74, no. 21, pp. 214405 – 1, 2006.

[52] Y. Tserkovnyak, A. Brataas, G. Bauer, and B. Halperin, "Nonlocal magnetization dynamics in ferromagnetic heterostructures," *Reviews in Modern Physics*, vol. 77, pp. 1375 – 421, 2005.

[53] P. Wolf, "Free oscillations of the magnetization in permalloy films," *Journal of Applied Physics*, vol. 32, no. 3, pp. S95–S96, 1961.

[54] T. Silva, C. Lee, T. Crawford, and C. Rogers, "Inductive measurement of ultrafast magnetization dynamics in thin-film permalloy," *Journal of Applied Physics*, vol. 85, pp. 7849–62, June 1999.

[55] A. Kos, T. Silva, and P. Kabos, "Pulsed inductive microwave magnetometer," *Review of Scientific Instruments*, vol. 73, p. 3563, 2002.

[56] M. R. Freeman, "Picosecond pulsed-field probes of magnetic systems (invited)," *Journal of Applied Physics*, vol. 75, no. 10, pp. 6194–6198, 1994.

[57] S. E. Russek, S. Kaka, and M. Donahue, "High-speed dynamics, damping, and relaxation times in submicrometer spin-valve devices," *Journal of Applied Physics*, vol. 87, pp. 7070–3, May 2000.

[58] E. Stoner and E. Wohlfarth, "A mechanism of magnetic hysteresis in heterogeneous alloys," *Philosophical Transactions of the Royal Society A*, vol. 240, pp. 599–642, 1948.

[59] A. Thiaville, "Extensions of the geometric solution of the two-dimensional coherent magnetization rotation model," *Journal of Magnetism and Magnetic Materials*, vol. 182, pp. 5–18, 1998.

[60] L. Neel, "Some theoretical aspects of rock-magnetism," *Advances in Physics*, vol. 4, pp. 191 – 243, 1955.

[61] W. Wernsdorfer, E. B. Orozco, K. Hasselbach, A. Benoit, B. Barbara, N. Demoncy, A. Loiseau, H. Pascard, and D. Mailly, "Experimental evidence of the néel-brown model of magnetization reversal," *Phys. Rev. Lett.*, vol. 78, pp. 1791–1794, Mar 1997.

[62] N. D. Rizzo, M. DeHerrera, J. Janesky, B. Engel, J. Slaughter, and S. Tehrani, "Thermally activated magnetization reversal in submicron magnetic tunnel junctions for magnetoresistive random access memory," *Applied Physics Letters*, vol. 80, no. 13, pp. 2335–2337, 2002.

[63] R. H. Koch, G. Grinstein, G. A. Keefe, Y. Lu, P. L. Trouilloud, W. J. Gallagher, and S. S. P. Parkin, "Thermally assisted magnetization reversal in submicron-sized magnetic thin films," *Phys. Rev. Lett.*, vol. 84, pp. 5419–5422, Jun 2000.

[64] J. Z. Sun, J. C. Slonczewski, P. L. Trouilloud, D. Abraham, I. Bacchus, W. J. Gallagher, J. Hummel, Y. Lu, G. Wright, S. S. P. Parkin, and R. H. Koch, "Thermal activation-induced sweep-rate dependence of magnetic switching astroid," *Applied Physics Letters*, vol. 78, no. 25, pp. 4004–4006, 2001.

[65] J. Z. Sun, "Spin-current interaction with a monodomain magnetic body: A model study," *Phys. Rev. B*, vol. 62, pp. 570–578, Jul 2000.

[66] J. Slonczewski, "Current-driven excitation of magnetic multilayers," *Journal of Magnetism and Magnetic Materials*, vol. 159, no. 1-2, pp. 1 – 7, 1996.

[67] Y. B. Bazaliy, B. Jones, and S.-C. Zhang, "Modification of the landau-lifshitz equation in the presence of a spin-polarized current in colossal- and giant-magnetoresistive materials," *Physical Review B (Condensed Matter)*, vol. 57, no. 6, pp. R3213–7, 1998.

[68] S. Petit, C. Baraduc, C. Thirion, U. Ebels, Y. Liu, M. Li, P. Wang, and B. Dieny, "Spin-torque influence on the high-frequency magnetization fluctuations in magnetic tunnel junctions," *Physical Review Letters*, vol. 98, no. 7, pp. 077203 – 1, 2007.

[69] S. Petit, N. de Mestier, C. Baraduc, C. Thirion, Y. Liu, M. Li, P. Wang, and B. Dieny, "Influence of spin-transfer torque on thermally activated ferromagnetic resonance excitations in magnetic tunnel junctions," *Physical Review B (Condensed Matter and Materials Physics)*, vol. 78, no. 18, pp. 184420 (13 pp.) –, 2008.

[70] *Ukranian Journal of Physics*, vol. 53, pp. 14–22, 2008.